Nonlinear Seismic Response of Earth Dams with Canyon Interaction

Angeliki Papalou, M.ASCE,[1] and Jacobo Bielak, M.ASCE[2]

Abstract: This paper examines the nonlinear earthquake response of earth dams, using a model that considers the deformability of the surrounding medium and effects of spatial variation of the seismic excitation. A finite-element based method has been developed in which the dam is idealized as a shear beam and the surrounding medium as a halfspace. Nonlinear behavior of the dam is modeled using multiyield surface plasticity theory. The model can simulate canyons of arbitrary shape and SH-wave seismic excitation. The methodology is illustrated by simulating the upstream–downstream earthquake response of La Villita Dam, which is located near the epicenter of the 1985 Mexico earthquake. Results show that the reduction in the response that occurs as a result of dam-canyon interaction remains significant when the inelastic deformation of the dam is included in the model, and that when examined in the frequency domain, nonlinearity has radically different effects at low, medium, and high frequencies of excitation.

DOI: 10.1061/(ASCE)1090-0241(2004)130:1(103)

CE Database subject headings: Dams, earth; Earthquakes; Seismic response; Finite elements; Canyons; Dam foundations.

Introduction

In a previous study (Papalou and Bielak 2001), the writers presented a finite element numerical procedure for evaluating the elastic seismic response to SH-wave earthquake excitation of earth and rockfill dams, including dam–canyon interaction effects. A model of La Villita Dam was selected to illustrate the effects of the flexibility of the canyon and energy loss due to radiation on the earthquake response of the dam. Overall, the results of the simulation showed that when the canyon is assumed to be rigid, the response of the dam tends to be higher than if dam–canyon interaction effects are taken into consideration. This observation suggests that including such interaction effects in the design process might prevent unnecessary conservatism. The main objective of the present study is to incorporate the inelastic behavior of the dam into the analysis and to examine how this behavior affects the earthquake response of the dam–canyon–foundation system.

Several different models have been considered for analyzing the nonlinear response of earth dams during earthquakes. They include, e.g., a one-dimensional (1D) hysteretic wedge (Elgamal et al. 1985); 2D and 3D finite element models subjected to various types of excitation (Prevost et al. 1985); a combined analytical–numerical 2D model involving an inhomogeneous shear wedge in a rectangular canyon (Elgamal 1987); and a simplified procedure for 3D inhomogeneous, one-zoned earth dams (Abdel-Ghaffar et al. 1987), which was subsequently used to analyze the seismic response of the Santa Felicia Dam (Elgamal et al. 1987a,b). All these models assume that the base of the dam is rigid. The effect of the dam alluvial foundation and the canyon geometry, but not dam–canyon interaction effects, were later incorporated in a study of the 3D elastoplastic response of the La Villita Dam (Elgamal 1992). More recently, Abouseeda and Dakoulas (1998) developed a coupled boundary element–finite element formulation for studying nonlinear seismic soil–structure interaction in two dimension and applied this formulation to an idealized heterogeneous earth dam founded directly on an elastic half space. All the aforementioned models have in common that the effect of the canyon is either ignored or the canyon is assumed to be rigid. On the other hand, studies that include dam–canyon interaction have largely been restricted to the linear range of behavior. A list of references on linear dam–canyon interaction may be found in Abouseeda and Dakoulas (1998) and in Papalou and Bielak (2001).

In this paper the method of analysis developed in Papalou and Bielak (2001), which henceforth will be referred to as Paper I, is extended to the nonlinear range in order to examine simultaneously the effects of dam–canyon interaction and of the inelastic deformation of the dam on earthquake response. The methodology is then used to model the earthquake response of the La Villita Dam and to compare the results with those from the earlier linear analysis. One important question that will be addressed is whether the coupling between the dam and the foundation remains significant when the inelastic deformation of the dam is included in the model.

Analysis of System

The seismic analysis of earth dams is complicated due to the many factors that influence their response. For this reason, several simplifying assumptions are generally made. In this study of the effects of dam–canyon interaction on earthquake dam response,

[1]Assistant Professor, Dept. of Engineering, Robert Morris Univ., Pittsburgh, PA 15108.

[2]Professor and Director, Dept. of Civil and Environmental Engineering, Computational Mechanical Laboratory, Carnegie Mellon Univ., Pittsburgh, PA 15213.

Note. Discussion open until June 1, 2004. Separate discussions must be submitted for individual papers. To extend the closing date by one month, a written request must be filed with the ASCE Managing Editor. The manuscript for this paper was submitted for review and possible publication on August 5, 2002; approved on February 11, 2003. This paper is part of the ***Journal of Geotechnical and Geoenvironmental Engineering***, Vol. 130, No. 1, January 1, 2004. ©ASCE, ISSN 1090-0241/2004/1-103–110/$18.00.

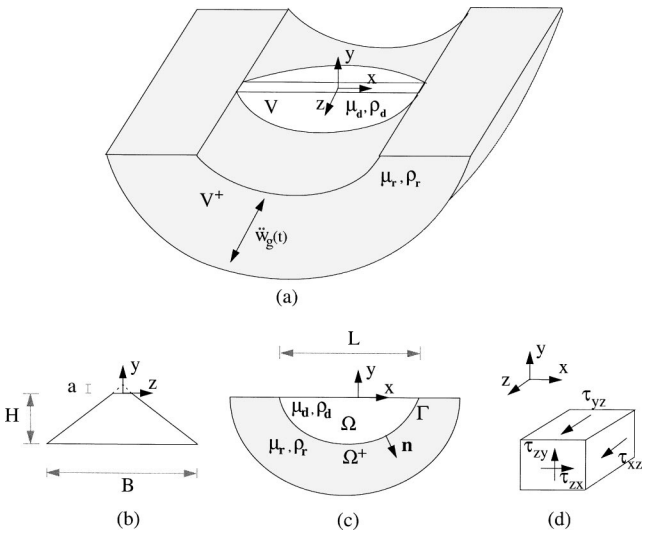

Fig. 1. Dam-canyon model: (a) three-dimensional view; (b) cross section of dam along transverse direction; (c) cross section of dam and canyon in longitudinal direction; and (d) shear stresses at point

the excitation is along the upstream–downstream direction and consists of SH-incident plane waves. Even though the input motion has a component only in one direction, for the case of inelastic material behavior the components of particle motion in the plane perpendicular to that direction do not vanish, as they do in the elastic case. Because of the initial stress state and the inelastic behavior, antiplane strain motions (in the upstream–downstream direction) are not uncoupled from plane strain motions parallel to the longitudinal axis of the dam. However, in a study of an idealized earth dam, also subjected to antiplane excitations, Joyner (1975) found that the peak plane strain components did not exceed 3% of the peak antiplane strain components. He also found that computations made with zero initial stresses did not differ significantly from those in which geostatic stresses were considered. Thus, in this study the dam is modeled as a shear beam of inhomogeneous inelastic material in which only transverse displacements and shear deformations are significant and geostatic stresses are implicitly considered only to determine the initial moduli of the dam material. The surrounding medium is modeled as an elastic halfspace (Fig. 1). This model is similar to that in Paper I, except that here the material in the dam obeys an inelastic constitutive law, to be specified later in this section. The canyon is of arbitrary shape and the dam can be inhomogeneous with varying density, ρ_d, and shear wave velocity, v_d. The homogeneous rock medium surrounding the canyon has density, ρ_r, and shear wave velocity, v_r. The corresponding shear moduli are $\mu_d = v_d^2 \rho_d$ and $\mu_r = v_r^2 \rho_r$ for the dam and rock medium, respectively. The dam is assumed to be bonded to the canyon at the interface Γ. Under the shear beam idealization, the only nonzero displacement is the transverse displacement $w(x,y,t)$ in the z direction. Therefore, the only nonvanishing strains are the shear strains γ_{xz}, γ_{zx}, γ_{yz}, γ_{zy}

$$\gamma_{xz} = \gamma_{zx} = \frac{\partial w}{\partial x} \tag{1}$$

$$\gamma_{yz} = \gamma_{zy} = \frac{\partial w}{\partial y} \tag{2}$$

and the corresponding shear stresses are τ_{xz} and τ_{yz}.

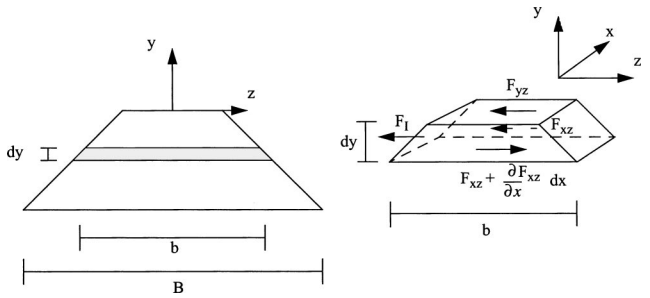

Fig. 2. Infinitesimal element of dam model and free-body diagram showing resultant forces on that element

To derive the equations of motion an infinitesimal element of the dam is considered (Fig. 2). The forces acting on the element during free vibrations include the inertia force F_I and the shear forces F_{xz} and F_{yz}, where

$$F_I = \rho b \, dy \, dx \, \ddot{w} \tag{3}$$

$$F_{xz} = \left(\int_{-b/2}^{b/2} \tau_{xz} \, dz \right) dy \tag{4}$$

$$F_{yz} = \left(\int_{-b/2}^{b/2} \tau_{yz} \, dz \right) dx \tag{5}$$

in which b = width of the dam at depth y and is given by $b = B\hat{h}$ where

$$\hat{h} = \frac{a-y}{a+H}$$

where a = distance from the vertex of crest to the crest of the dam, and H = height of dam.

Equilibrium of the forces acting on the element in the z direction yields the following equation of motion:

$$\rho_d b \ddot{w} - \frac{\partial b \tau_{xz}}{\partial x} - \frac{\partial b \tau_{yz}}{\partial y} = 0 \tag{6}$$

The equation of motion and interface conditions can be written in the following form:

$$\hat{\rho}_d \ddot{w} - \nabla \cdot (\hat{h}\tilde{\tau}) = 0 \quad \text{in } \Omega \tag{7}$$

$$\rho_r \ddot{w} = \mu_r \nabla^2 w = 0 \quad \text{in } \Omega^+ \tag{8}$$

$$\hat{h}\tilde{\tau} \cdot n = \mu_r \nabla w \cdot n \quad \text{on } \Gamma \tag{9}$$

where

$$\tilde{\tau} = \begin{Bmatrix} \tau_{xz} \\ \tau_{yz} \end{Bmatrix}$$

where $\hat{\rho}_d$ = effective mass density given by $\hat{\rho}_d = \rho_d \hat{h}$; ∇ = gradient operator; and n = outward unit normal vector at the interface Γ directed from Ω to Ω^+. Eqs. (7) and (8) are the equations of motion within the dam and the exterior region, respectively. Eq. (9) represents the continuity of traction across the dam–canyon interface, Γ. In addition, the displacement w is required to be continuous across Γ, since the dam and the surrounding medium are assumed to be bonded at this interface. In the derivation of Eqs. (8) and (9), use has been made of the linear relationship between stress and strain in the region outside the dam

J. Geotech. Geoenviron. Eng., 2004, 130(1): 103-110

$$\tau_{iz}=\tau_{zi}=\mu_r\gamma_{iz}, \quad i=x,y \text{ in } \Omega^+ \tag{10}$$

since the material in Ω^+ is linearly elastic.

Nonlinear Constitutive Law

To describe the nonlinear behavior of the dam material, a two-dimensional shear model based on the multiyield surface plasticity theory is used (Prevost 1977). In this model a family of nested circular yield surfaces is introduced. A kinematic hardening rule is used to specify the evolution of the loading surface. During the course of the plastic deformations yield surfaces translate in stress space by the stress point without changing in shape; they touch and push each other but they do not intersect. Each yield surface is associated with a plastic shear modulus which can be obtained from an experimental shear stress–strain curve. In this study the experimental shear stress–strain curve for each material comprising the dam was approximated by the hyperbolic equation

$$\tau=G_0\frac{\gamma}{1+\dfrac{\gamma}{\gamma_r}} \tag{11}$$

where G_0=elastic shear modulus; γ_r=reference strain; τ=shear stress; and γ=associated shear strain. The maximum shear stress is chosen to be $G_0\gamma_r$.

The skeleton stress–strain curve is approximated by linear segments along which the tangent modulus H is constant. Each linear segment is associated with a yield surface with shear elastoplastic modulus H (Elgamal et al. 1987a,b).

The yield criterion is represented by an equation of the following form:

$$f^{(m)}=(\tau_{\beta z}-\alpha_{\beta z}^{(m)})(\tau_{\beta z}-\alpha_{\beta z}^{(m)})-(R^{(m)})^2=0 \tag{12}$$

in which a Greek subscript takes the values x and y; a repeated Greek subscript denotes summation; $R^{(m)}$=radius of the yield surface m; and α=offset of the surface with respect to the origin.

Based on the above equation, the associative flow rule, and the kinematic hardening rule, the incremental elasto–plastic stress–strain relation is represented by

$$\dot{\tau}_{\beta z}=G_0\dot{\gamma}_{\beta z}-\left(G_0-\frac{1}{2}H^{(m)}\right)\times\frac{\tau_{\beta z}-\alpha_{\beta z}^{(m)}}{(R^{(m)})^2}(\tau_{\kappa z}-\alpha_{\kappa z}^{(m)})\dot{\gamma}_{\kappa z} \tag{13}$$

The problem defined by Eqs. (1)–(13) plus the displacement continuity condition across Γ is solved by the finite element method using standard Galerkin ideas for spatial discretization in terms of the displacement w. The particular method used for formulating the numerical model for the current study is essentially that of Paper I, with a modification to handle nonlinearity. It uses quadratic six-node subparametric triangular elements with 1 degree of freedom per node. The formulation uses the numerical treatment of Kallivokas et al. (1991) for limiting spurious wave reflections at the truncated boundary, and the effective input forces of Bielak and Christiano (1984) to incorporate the seismic motion into the computational domain.

The assembly of the element matrices leads to a system of equations of the form

$$M\ddot{w}+p=f \tag{14}$$

in which M=global mass matrix; w=vector of time-dependent nodal displacements; f=time-varying vector representing the effective nodal forces; and p=time-varying nonlinear internal force vector, given by

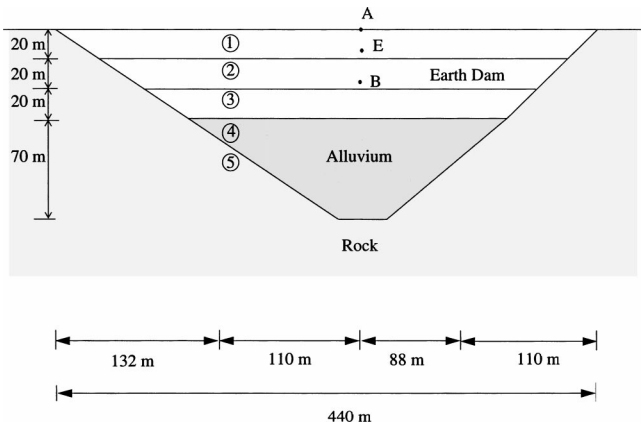

Fig. 3. Geometry of La Villita dam model

$$p=\int_\Omega B^T\tilde{\tau}\,d\Omega \tag{15}$$

where B=the strain–displacement matrix; and $\tilde{\tau}$=stress vector (determined from the soil constitutive model).

Eq. (15), with the system initially at rest, is solved using the predictor–corrector form of the Newmark scheme which consists of the following equations (Owen and Hinton 1980):

$$M\ddot{w}_{n+1}+p_{n+1}=f_{n+1} \tag{16}$$

$$w_{n+1}=\tilde{w}_{n+1}+\Delta t^2\beta\ddot{w}_{n+1} \tag{17}$$

$$\dot{w}_{n+1}=\tilde{\dot{w}}_{n+1}+\Delta t\gamma\ddot{w}_{n+1} \tag{18}$$

where

$$\tilde{w}_{n+1}=w_n+\Delta t w_n+\frac{\Delta t^2}{2}(1-2\beta)\ddot{w}_n \tag{19}$$

$$\tilde{\dot{w}}_{n+1}=\dot{w}_n+\Delta t(1-\gamma)\ddot{w}_n \tag{20}$$

where Δt=time step; β and γ=free parameters which control the accuracy and stability of the method ($\beta=0.25,\gamma=0.5$); $\tilde{w}_{n+1}$ and $\tilde{\dot{w}}_{n+1}$=predictor values; and w_{n+1} and $\dot{w}_{n+1}$=corrector values.

Nonlinear Seismic Response of La Villita Dam

This section is devoted to modeling the nonlinear seismic response of La Villita Dam, an earth and rockfill dam located in the epicentral region of the 1985 Mexico earthquake, and to comparing this response with that obtained from a linear analysis. This dam experienced inelastic deformation but suffered no significant damage during that earthquake (Elgamal 1992). The geometry and material properties of the dam have been reported by Elgamal et al. (1990), Elgamal (1992). The idealized dam–canyon model considered in the present investigation is the same as that utilized in Paper I, except that here the dam is allowed to behave inelastically. Fig. 3 and Table 1 present the geometry and the idealized elastic material properties used. Damping is 5% critical in the dam material and 0.5% in the halfspace. The nonlinear behavior of the dam materials was modeled using a multiyield surface plasticity theory as mentioned earlier in the description of the constitutive law used in the analysis. The plastic shear modulus associated with each yield surface was obtained using the hyperbolic Eq. (11). The value of the reference strain γ_r was considered constant and equal to 0.0013. Pore water pressure effects

J. Geotech. Geoenviron. Eng., 2004, 130(1): 103-110

Table 1. Elastic Material Properties of Model of La Villita Dam

Material	Mass density (kg/m^3)	Shear wave velocity (m/s)
1	2,100	275
2	2,100	310
3	2,100	335
4	2,100	300
5	2,300	variable

were not directly taken into consideration. These will contribute to further amplify the effects of nonlinearity. An accelerogram of horizontal ground motion recorded at an abutment of La Villita Dam during the September 19, 1985 Mexico earthquake is used as input motion (Fig. 4). The incoming seismic waves are taken to be vertically incident, with an amplitude half of that of the recorded seismogram, and polarized in the antiplane direction of the dam. Numerical solutions are satisfactory provided the mesh contains a minimum of about nine points per wavelength. The finite element mesh used for solving this problem is the same as that used in Paper I. This mesh can represent frequencies up to 3.5 Hz with negligible error and less than 20% error for frequencies up to 5 Hz.

Transient Response of Dam

In Paper I it was found that the dynamic interaction between the dam and the canyon is significant for the elastic seismic response of the dam. This behavior is illustrated in Fig. 5, which shows the synthetic accelerograms at the midcrest of the dam (Fig. 3, point A) for three different values of the shear wave velocity, v_r, in the rock. The first accelerogram from the top is for $v_r=4{,}000$ m/s, used to represent a very hard rock, such as granite. This corresponds to a case in which all the points at the interface of the dam and the canyon experience essentially identical motion, with little energy escaping into the exterior domain. The next accelerogram down is for $v_r=2{,}000$ m/s, a value that represents sound rock, and the third one, for $v_r=1{,}000$ m/s, represents a weathered rock. The corresponding impedance ratios between the exterior medium surrounding the canyon and the dam and alluvium material are 14.6, 7.3, and 2.7 respectively. The recorded motion at the same location is shown at the bottom of Fig. 5. The spikes that appear in the recorded acceleration are thought to be a consequence of a stick–slip displacement mechanism in the zone below the crest strong-motion instrument. At the end of each slip phase, a sudden change in inertial load may occur and cause a spike to appear in the acceleration record (Elgamal 1992). These spikes have much higher frequencies than those that can be represented with the finite element mesh used for the present simulations. The recorded motion also shows lower dominant frequencies than those exhibited by the synthetic accelerograms at the midcrest. A comparison of the three synthetic seismograms in Fig. 5 shows a distinct reduction in the response with a decrease in v_r, especially during the first 20 s. The reduction of the response within this range is 18 and 35% for $v_r=2{,}000$ and 1,000 m/s with respect to that for the very stiff base. Fig. 6 shows that the reduction in response is almost of the same order when the nonlinear dam behavior is taken into consideration. This indicates that dam–canyon interaction effects remain significant after the dam enters into the inelastic range. On the other hand, the extent of nonlinearity observed at midcrest is small; pair wise reduction between the accelerograms in Fig. 5 and the corresponding accelerogram in Fig. 6 is only on the order of 10–15%.

Figs. 7 and 8 are used to examine the response at an interior location within the dam. They show the synthetic accelerograms at point B (Fig. 3), about 40 m below the crest. At this location the nonlinear effects are more pronounced than at the crest, with a reduction in the peak values of about 30%, both for $v_r=4{,}000$

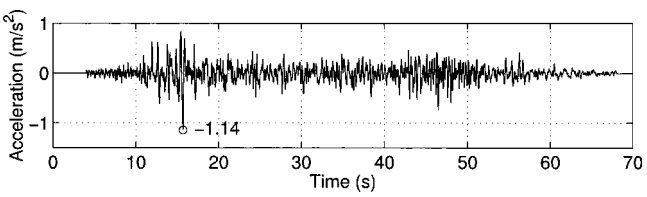

Fig. 4. Recorded free-field acceleration of September 19, 1985 Mexico earthquake used in simulations of transient response of La Villita dam model

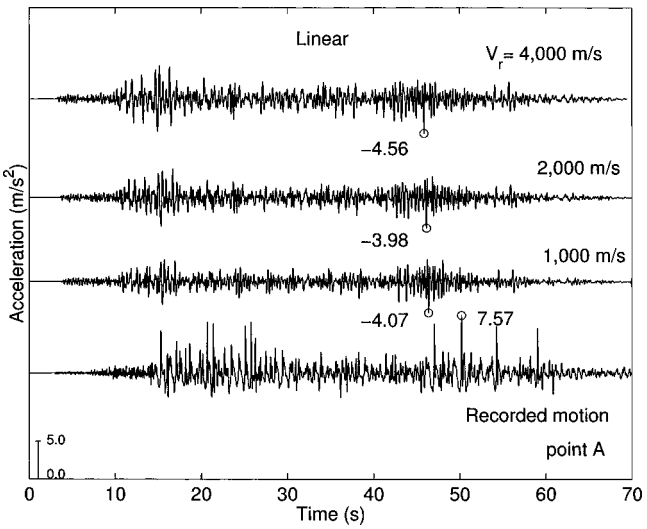

Fig. 5. Synthetic accelerograms at midcrest of linear dam model, for several values of shear wave velocity of rock base; and observed accelerogram at same point

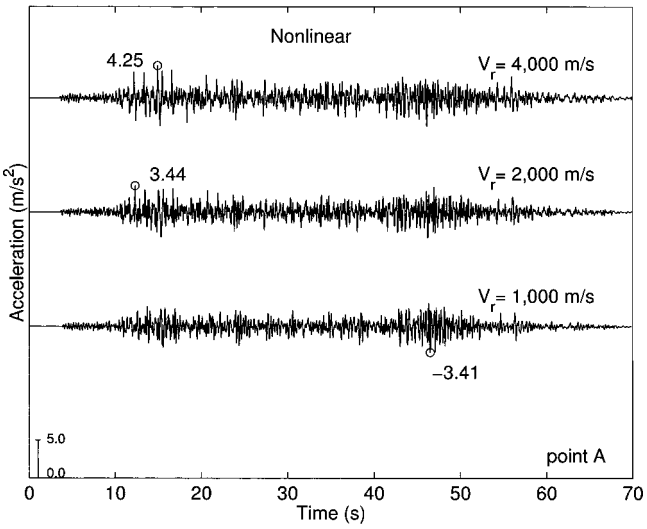

Fig. 6. Synthetic accelerograms at midcrest of nonlinear dam model, for several values of shear wave velocity of rock base

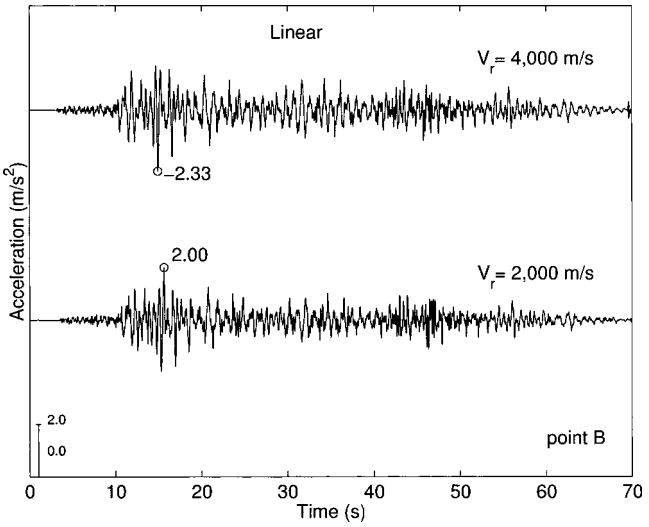

Fig. 7. Synthetic accelerograms at interior point B (Fig. 3) of linear dam model, for two values of shear wave velocity of rock base

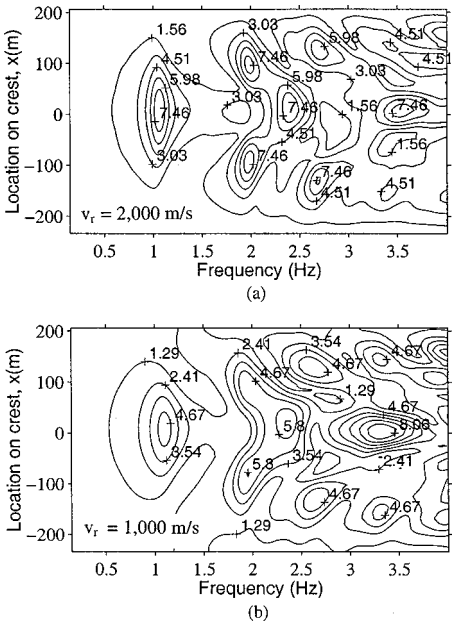

Fig. 9. Amplitude of transfer function of linear dam response along crest with respect to free-field steady-state harmonic excitation, for two values of shear wave velocity of rock base

and 2,000 m/s. Also the effects of dam–canyon interaction are strong for the inelastic dam: the reduction of peak amplitude of the dam, between the softest and the stiffest canyon is of 40%. It is also noteworthy that the dominant periods of oscillation are longer at B than at midcrest. They are similar to those observed in the recorded accelerogram at the bottom of Fig. 5.

Frequency Response Analysis

To gain further insight into the reasons for the differences in behavior described in the preceding paragraphs, it is useful to examine the response of the dam in the frequency domain. Fig. 9 shows the amplitude of the transfer function of the response along the crest of the dam–canyon system with respect to the free-field response for the elastic dam for $v_r = 2{,}000$ and 1,000 m/s, considering elastic dam behavior. In each case the dam exhibits resonance at a discrete number of frequencies (1.1, 2.3, 3.3–3.5 Hz, etc.). For some of these frequencies, the largest response occurs near the middle of the dam, while for others it occurs near the edges. Fig. 10 shows the amplitude of the transfer function with depth, down the middle section (beneath point A in Fig. 3), for three resonant frequencies. These resonant shapes suggest that the midcrest can respond equally at all three frequencies. The actual response depends, of course, on the frequency content of the excitation. On the other hand, at the interior location B, the contribution from the higher resonant frequencies will be highly diminished, since the response decreases faster with depth than for the first resonance and almost vanishes at the higher frequencies. Thus, it is not surprising that the response at B exhibits longer dominant periods than at midcrest. In addition, the derivative with respect to depth vanishes at the free surface for all frequencies, in consonance with the requirement that the free surface be traction free; it varies more rapidly at depth for the higher resonance than for the fundamental resonant frequency; and assumes the largest values at some depth. Thus, the strains and therefore nonlinear effects can be expected to be more pronounced within this region.

The contribution to the total response from each frequency component can be more clearly analyzed by examining the power spectral density (PSD) of the various accelerograms. Figs. 11 and

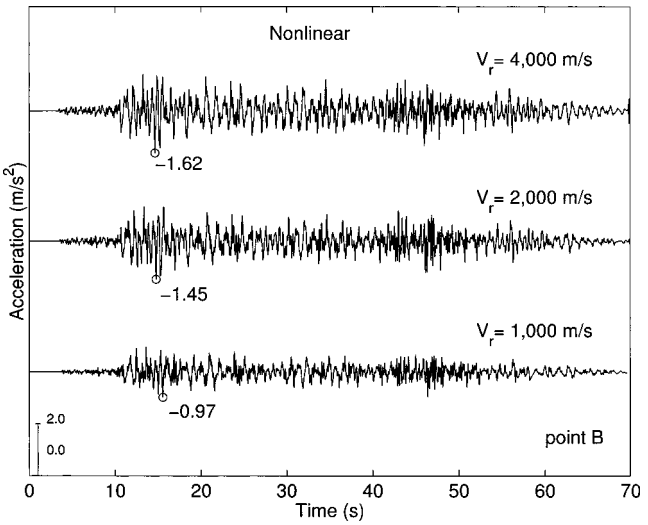

Fig. 8. Synthetic accelerograms at interior point B (Fig. 3) of nonlinear dam model, for several values of shear wave velocity of rock base

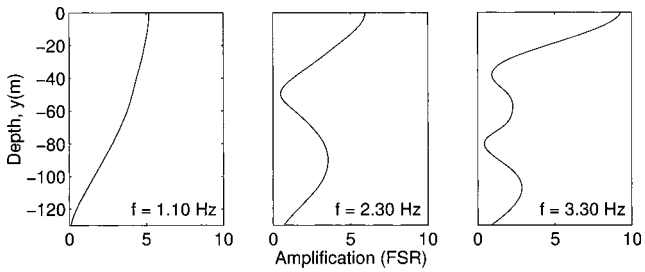

Fig. 10. Amplitude of transfer function of linear dam response, FSR, down middle section, with respect to free-field steady-state harmonic excitation, for three different resonant frequencies; $v_r = 1{,}000$ m/s

J. Geotech. Geoenviron. Eng., 2004, 130(1): 103-110

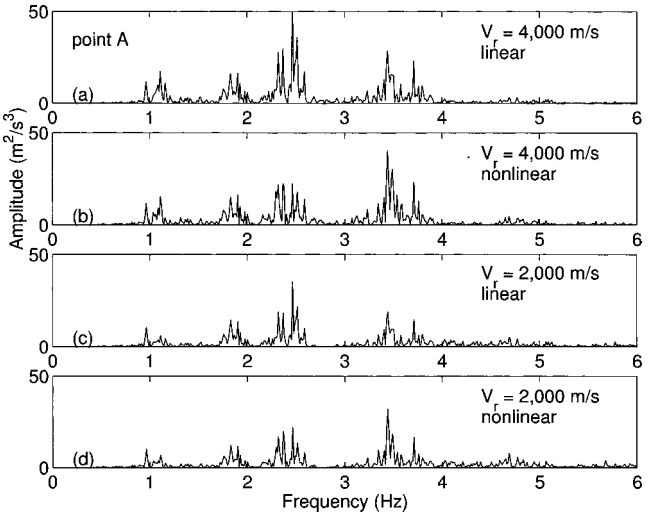

Fig. 11. Power spectral density of synthetic accelerogram at midcrest of linear and nonlinear models of dam, for several values of shear wave velocity of rock base

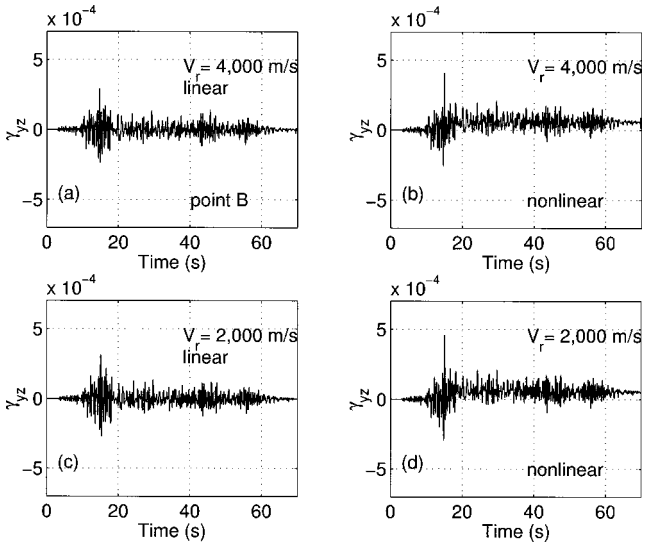

Fig. 13. Time history of shear strain γ_{yz} at point B (Fig. 3) of linear and nonlinear models of dam, for two values of shear wave velocity of rock base

12 show, respectively, the amplitude of the PSD at midcrest (Point A) and at the interior point B, for the linear and nonlinear cases, for two different shear wave velocities of the rock. These figures suggest that in the spectral domain the effect of the nonlinearity on the spectrum can be divided into several frequency bands. The relative contribution from the different frequency components is quite different at the two locations. The response at midcrest exhibits three distinct types of behavior (Fig. 11). At the lowest frequencies (<2 Hz), the spectral amplitudes are not affected by nonlinearity. In the intermediate frequencies, between 2 and 3 Hz, the power spectral density decreases as a consequence of nonlinearity; and at the higher frequencies, the spectral amplitudes increase relatively to the corresponding linear system due to the sharp reversals that occur as the soil material changes from the plastic to the elastic state. Yu et al. (1992) have observed an almost identical pattern for the free-field motion in a 1D analysis of nonlinear soil response during earthquakes. For the dam, this pattern remains true for the two cases of rock basement considered. Now, if instead of comparing linear versus nonlinear behavior, one considers the shear wave velocity of the material surrounding the canyon as a parameter, it will be seen that a new pattern appears. In this case, the spectral amplitude decreases with the decrease in shear wave velocity v_r, both for the linear and nonlinear cases.

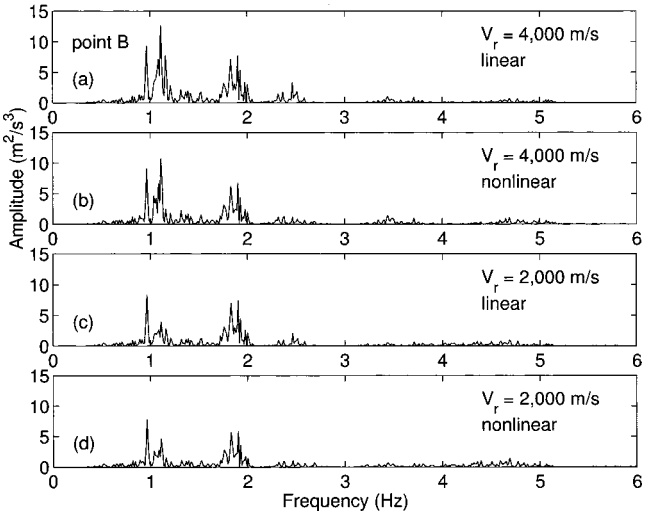

Fig. 12. Power spectral density of synthetic accelerogram at interior point B (Fig. 3) of linear and nonlinear models of dam, for several values of shear wave velocity of rock base

At the interior location B, the spectral amplitude shown in Fig. 12 differs from that at midcrest. First, the response at B is confined to the lower frequency range, since at the higher frequencies the corresponding resonant shapes almost vanish at that location (Fig. 10). Second, the largest changes in the response between the four different cases occur for frequencies near the first resonance. Here, nonlinearity causes a noticeable reduction for the stiffer canyon, and a small decrease for the softer one. Very large reductions occur both for the linear and the nonlinear cases with decreasing values of v_r.

Shear Strains–Shear Stresses

Besides accelerations, the earthquake performance of a dam depends on the strains and stresses it undergoes during the seismic event. In Paper I it was found that the maximum strain γ_{yz} occurs at points below the midcrest. Figs. 13 and 14 show the evolution of this strain with time at two interior points, B and E (Fig. 3), both for the linear and the nonlinear cases, for v_r=2,000 and 4,000 m/s. There are two main differences between the response of the elastic and inelastic cases. During the first 16 s the strains at B and E remain elastic; then, as a consequence of the large pulse in the input motion at that time (Fig. 4) there occurs a significant inelastic excursion. There is some additional inelastic deformation during the rest of the excitation, but most of the additional response is elastic. At the end of the excitation, there remains a small permanent deformation.

The sequence of the deformation can be clearly appreciated in Fig. 15, which shows the history of the stress versus strain at the same locations, for the inelastic dam. Notice that the permanent set, both at B and E, is greater for v_r=4,000 m/s than for the softer base, as less energy escapes through the canyon.

J. Geotech. Geoenviron. Eng., 2004, 130(1): 103-110

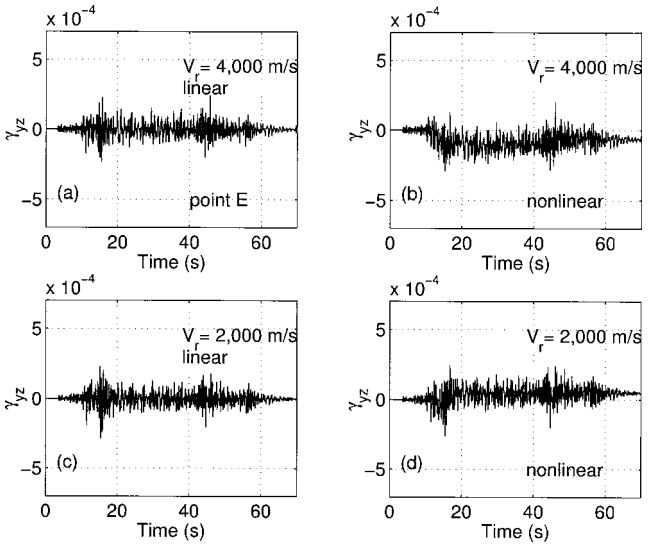

Fig. 14. Time history of shear strain γ_{yz} at point E (Fig. 3) of linear and nonlinear models of dam

Concluding Remarks

The present study was based on several simplifying assumptions and was applied to a single dam geometry and excitation. Nonetheless, several observations can be made from the present simulation of the inelastic response of the La Villita Dam to the 1985 Mexico earthquake. While the relative importance of different parameters will clearly vary for different applications, the overall qualitative behavior is expected to remain valid in more general situations.

The inclusion of the dam–canyon interaction effects into the analysis leads to a reduction of the acceleration response of the dam with respect to that in which the canyon is assumed to be rigid. This behavior occurs both for the linear and nonlinear cases. However, the effects of nonlinearity are most pronounced within the interior of the dam, where shear strains are largest. The reduction due to nonlinearity in the peak acceleration at a point 40 m below the crest of the dam is on the order of 25–30%, for a given canyon stiffness. Further, even with the softening of the dam due to inelastic deformation the effects of the flexibility of the canyon remain strong, e.g., for the soft canyon ($v_r = 1{,}000$ m/s), the peak value of the acceleration at the same point is about 40 percent less than for $v_r = 4{,}000$ m/s. When examined in the frequency domain, the power spectral density of the acceleration is qualitatively different for different bands. At midcrest, nonlinearity has no effect at low frequencies; it decreases the response at midrange; and produces an increase of the response at high frequencies. By contrast, within the interior of the dam, important reductions due to nonlinearity occur at low- and mid-range frequencies; the contribution is very small at higher frequencies, both for the linear and the nonlinear cases. On the other hand, the effects of dam–canyon interaction occur at all frequencies, both for the linear and the nonlinear cases. The shear strains in the dam behave elastically during the initial portion of the excitation. Later on, as a consequence of a large pulse in the input motion, there occurs a significant inelastic excursion. There is some additional inelastic deformation during the rest of the excitation, but most of the additional response is elastic. At the end of the excitation, there remains a small permanent deformation.

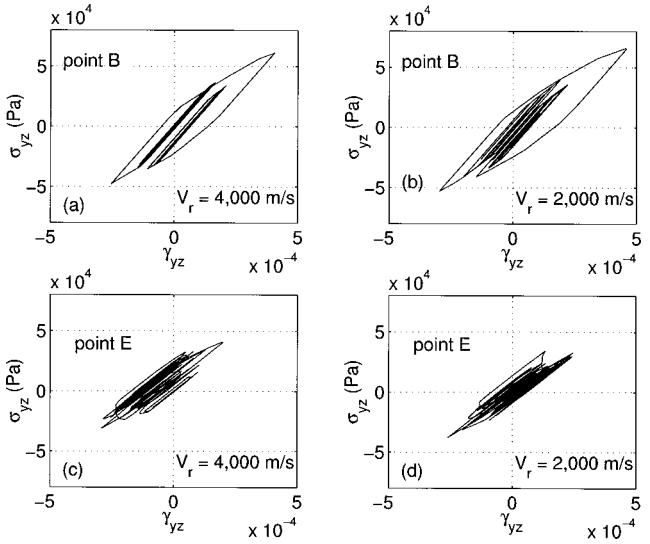

Fig. 15. History of stress–strain τ_{yz} versus γ_{yz} at interior points B and E (Fig. 3) of nonlinear dam model, for two values of shear wave velocity of rock base

Acknowledgments

This study was supported by a grant from the National Science Foundation (No. CMS-9320824). The cognizant program director was Dr. Clifford J. Astill. The writers are grateful for this support. The earthquake records were supplied by Universidad Nacional Autónoma de México (UNAM), with the help of Professor G. Ayala (UNAM) and Professor E. Mena (UNAM). Thanks also go to Professor A.-W. Elgamal for providing the writers with a copy of the accelerogram in Fig. 4.

References

Abdel-Ghaffar, A. M., and Elgamal, A.-W. (1987). "Elasto-plastic seismic response of 3-D earth dam: Theory." *J. Geotech. Eng.*, 113(11), 1293–1308.

Abouseeda, H., and Dakoulas, P. (1998). "Non-linear dynamic earth dam-foundation interaction using a BE-FE method." *Earthquake Eng. Struct. Dyn.*, 27, 917–936.

Bielak, J., and Christiano, P. (1984). "On the effective seismic input for non-linear soil-structure interaction systems." *Earthquake Eng. Struct. Dyn.*, 12, 107–119.

Elgamal, A.-W. (1992). "Three-dimensional seismic analysis of La Villita dam." *J. Geotech. Eng.*, 118(12), 1937–1958.

Elgamal, A.-W., Abdel-Ghaffar, A. M., and Prevost, J.-H. (1985). "Elasto-plastic earthquake shear-response of one-dimensional earth dam models." *Earthquake Eng. Struct. Dyn.*, 13, 617–633.

Elgamal, A.-W., Abdel-Ghaffar, A. M., and Prevost, J.-H. (1987a). "2-D elastoplastic seismic shear response of earth dams: Theory." *J. Eng. Mech.*, 113(5), 689–701.

Elgamal, A.-W., Abdel-Ghaffar, A. M., and Prevost, J.-H. (1987b). "2-D elastoplastic seismic shear response of earth dams: Applications." *J. Eng. Mech.*, 113(5), 702–719.

Elgamal, A. W., Scott, R. F., Succarieh, M. F., and Yan, L. (1990). "La Villita dam response during five earthquakes including permanent deformation." *J. Geotech. Eng.*, 116(10), 1443–1462.

Joyner, W. B. (1975). "A method for calculating nonlinear seismic response in two dimensions." *Bull. Seismol. Soc. Am.*, 65, 1337–1357.

Kallivokas, L. F., Bielak, J., and MacCamy, R. C. (1991). "Symmetric local absorbing boundaries in time and space." *J. Eng. Mech.*, 117(9), 2027–2048.

Owen, D. R. J., and Hinton, E. (1980). *Finite elements in plasticity: Theory and practice*, Pineridge Press Limited, Swansea, U.K.
Papalou, A., and Bielak, J. (2001). ''Seismic elastic response of earth dams with canyon interaction.'' *J. Geotech. Geoenviron. Eng.,* 127(5), 446–453.
Prevost, J. H. (1977). ''Mathematical modelling of monotonic and cyclic undrained clay behaviour.'' *Int. J. Numer. Analyt. Meth. Geomech.,* 1, 195–216.
Prevost, J. H., Abdel-Ghaffar, A. M., and Lacy, S. J. (1985). ''Nonlinear dynamic analyses of an earth dam.'' *J. Geotech. Eng.,* 111(7), 882–897.
Yu, G., Anderson, J. G., and Siddharthan, R. (1992). ''On the characteristics of nonlinear soil response.'' *Bull. Seismol. Soc. Am.,* 83, 218–244.